JACS JOURNAL OF THE AMERICAN CHEMICAL SOCIETY

COMMUNICATION

pubs.acs.org/JACS

A Metal−Insulator Transition in R_2O_2Bi with an Unusual Bi^{2-} Square Net (R = Rare Earth or Y)

Hiroshi Mizoguchi[†] and Hideo Hosono[*,†,‡]

[†]Frontier Research Center and [‡]Materials and Structures Laboratory, Tokyo Institute of Technology, 4259 Nagatsuta, Midori-ku, Yokohama 226-8503, Japan

Supporting Information

ABSTRACT: A series of tetragonal $ThCr_2Si_2$-type compounds, R_2O_2Bi (R = rare earth or Y), are synthesized in which an unusual Bi^{2-} anion forms a square net layer that is sandwiched between $(R_2O_2)^{2+}$ fluorite layers. Two-dimensional (2D) electronic bands around the Fermi energy are predominantly composed of $6p_x6p_y$ orbitals in the Bi^{2-} square net, which contains a positive hole per Bi^{2-} ion. The decrease in the size of the square net caused by reducing the size of the R ion enhances the electrical conductivity because of the hole, resulting in a "chemical pressure"-induced metal−insulator transition.

Ions with an unusual valence state are an important constituent in the realization of electronically active functions in solids. Typical examples are cuprates or iron pnictides heavily doped with carriers for high temperature superconductivity.[1] Transition metal ions can adopt complicated positively charged states, whereas heavy main group elements alter their valence state from positive (cationic) to negative (anionic) depending on their chemical environment. Bi usually adopts a closed shell electronic configuration in compounds, and trivalent ($6s^26p^0$), pentavalent ($6s^06p^0$), and −3 valent ($6s^26p^6$) are representative valence states. Nonconventional cationic valence states are stabilized by the aid of lattice vibration in perovskite-type oxides such as $Ba(Pb_{1-x}Bi_x)O_3$ and $(Ba_{1-x}K_x)BiO_3$, and these metallic oxides show superconductivity with T_c of 10−30 K.[2] On the other hand, anionic Bi is observed in solids containing electropositive elements.[3] Bi^- ions often form a square net in solids.[4−7] For example, $LaLiBi_2$ with ZrCuSiAs-type can be represented as $La^{3+}Li^+Bi^{3-}Bi^-$.[6] Bi^- with a $6s^26p^4$ electronic configuration forms a square net with a Bi−Bi distance of ∼3.2 Å, and contains two positive holes in the Bi 6p band, resulting in the formation of a metallic state. Recently, a superconducting transition at T_c = 4 K has been reported for $CeNi_xBi_2$ with the same crystal structure.[8] The synthesis of Ce_2O_2Bi was first reported in 1971 by Benz.[9] Very recently, Nuss and Jansen reported the synthesis of Pr_2O_2Bi.[10] These compounds contain Bi^{2-} if the lanthanide ions assume a trivalent state. In this communication, we report the synthesis of R_2O_2Bi (R = La−Er, or Y) and the metal−insulator transition (MIT) of these materials. These compounds contain a Bi^{2-} square net, and the delocalization of a positive hole in the Bi 6p band induces the MIT upon the application of chemical pressure.

Polycrystalline samples of R_2O_2Bi (R = La, Ce, Pr, Nd, Sm, Eu, Gd, Ho, Er, Yb, and Y) were synthesized by solid-state reaction at elevated temperature in evacuated silica ampules.

The starting materials used were R (R = La, Ce, Pr, Nd, Sm, Eu, Gd, Ho, Er, Yb, and Y, 99.9%), R_2O_3 (R = La, Nd, Sm, Eu, Gd, Ho, Er, Yb, and Y. 99.9%), CeO_2 (99.9%), Pr_6O_{11} (99.9%), and Bi (99.9%). Rare earth oxides were heated at 1273 K for 10 h before weighing. Appropriate amounts of these reagents were heated in an evacuated silica ampule at 773 K for 10 h, followed by heat treatment at 1023 K for 20 h. The products obtained were ground, pressed into pellets, and then heated in an evacuated silica ampule at 1273 K for 20 h. All of the starting materials were handled in an Ar-filled glovebox (O_2, H_2O <1 ppm). All of the obtained pellets were black. The crystal structures of the synthesized materials were examined by powder X-ray diffraction (XRD; Bruker D8 Advance TXS) using Cu Kα radiation[11] with the aid of Rietveld refinement using Code TOPAS3.[12] X-ray data were collected in the range of 2θ = 10−100° at 0.02° intervals at room temperature.

The powder XRD spectrum of La_2O_2Bi (Figure 1) identified the tetragonal phase of La_2O_2Bi and a residual amount of La_2O_3. The crystal structure of La_2O_2Bi was refined using Rietveld structure analysis based on a $ThCr_2Si_2$-type structure with the space group *I4/mmm* (No. 139), and the structure of La_2O_2Bi is shown in Figure 1. The estimated amount of La_2O_3 was 5.2 mol %. The refined structural parameters for La_2O_2Bi, together with other R_2O_2Bi compounds (R = Y, Nd, Sm, Gd, Ho, Er) are summarized in Table S1, and some bond distances and angles for these compounds are given in Table S2. In the crystal structure of La_2O_2Bi, each O ion coordinates with four La ions to form a fluorite layer, La_2O_2. The La_2O_2 and Bi layers are alternately stacked along the *c*-axis, and the Bi ion occupies a 2a site with D_{4h} site-symmetry, resulting in the formation of a Bi square net. Note that the Bi−Bi distance is 4.08 Å (that is, the *a*-value), which is much longer than that observed for square nets of Bi^- (∼3.2 Å).[4−6] The compound with R = Ce decomposes exothermically when exposed to an ambient atmosphere. Eu and Yb do not form the R_2O_2Bi phase. Figure 2 shows the variation in lattice constants and unit cell volume with the R ion. The unit cell volumes change monotonically with the atomic number of the R ion in accordance with the lanthanide contraction rule, suggesting that each R ion adopts the +3 charged state in the R_2O_2Bi compounds synthesized here. This indicates that the Bi ion in the square net has a −2 charge, which is a very unusual valence state

Received: December 8, 2010
Published: February 8, 2011

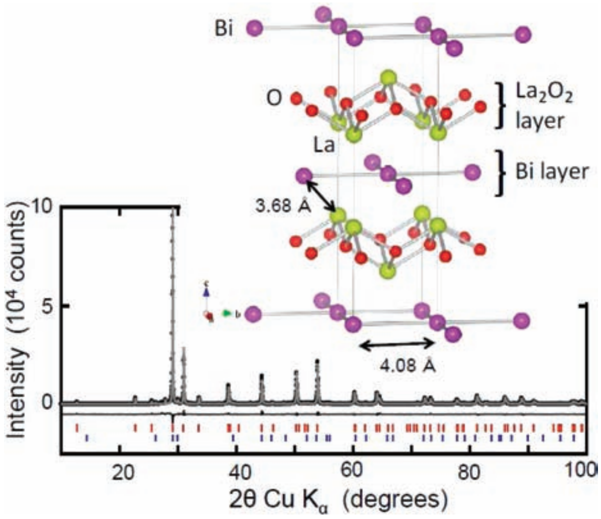

Figure 1. (Bottom) XRD pattern of La_2O_2Bi as measured (black dots) and refined by the Rietveld method (gray line). The vertical bars at the bottom show the calculated positions of the Bragg diffractions of La_2O_2Bi (upper), and La_2O_3 (lower). (Top) Obtained crystal structure of La_2O_2Bi. La_2O_2 and Bi layers are alternately stacked along the *c*-axis.

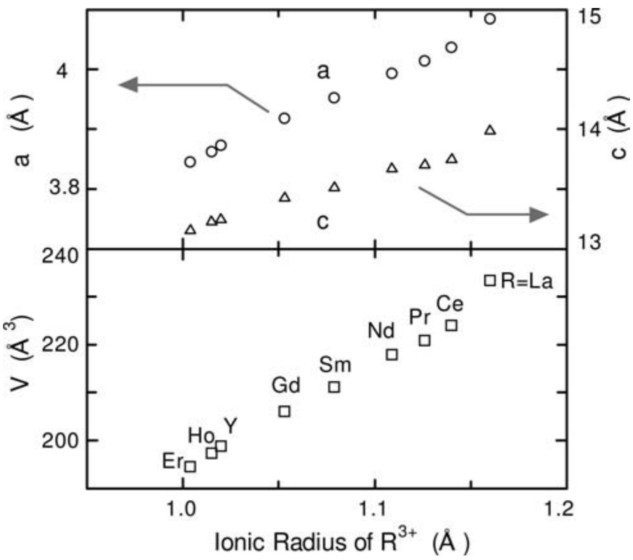

Figure 2. Cell edges and unit cell volume of R_2O_2Bi compounds estimated from X-ray Rietveld refinements. The data for Ce_2O_2Bi and Pr_2O_2Bi are taken from the report by Nuss and Jansen.[10] The ionic radius of R^{3+} ion reported by Shannon[13] is used.

for Bi. For Ce_2O_2Bi, a small deviation from the average curve suggests partial oxidation of the Ce ions to Ce^{4+}. As the size of the R ion decreases, it systematically shifts toward the O layer, and the OR_4 tetrahedron is compressed along the *c*-axis. The *a*-value corresponding to the Bi—Bi distance in the *ab* plane changes from 4.08 Å for La_2O_2Bi to 3.85 Å for Er_2O_2Bi.

Figure 3 shows the electronic band structure (E-k diagram) and density of states (DOS) of La_2O_2Bi obtained from a linear muffin tin orbital (LMTO) calculation developed by Andersen and co-workers.[14] The Fermi energy (E_F) crosses two bands along the ΓX line, suggesting a metallic nature. The partial DOS provides the following information about the chemical bonds in

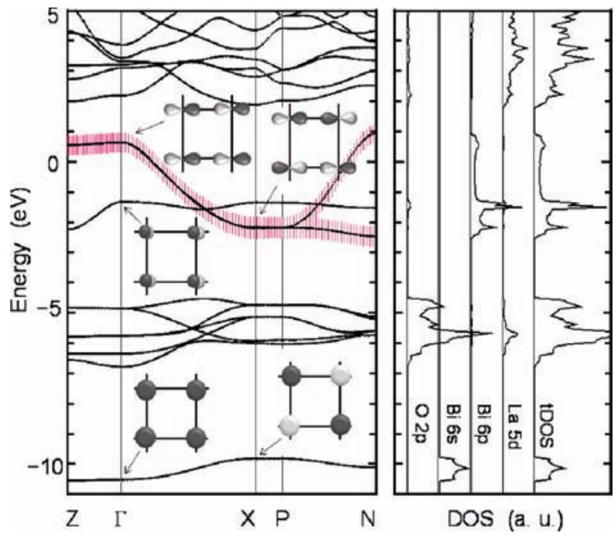

Figure 3. Band structure diagram for La_2O_2Bi. Γ = (0,0,0), *Z* = (1/2, 1/2, −1/2), *X* = (0, 0, 1/2), *P* = (1/4, 1/4, 1/4), and *N* = (0, 1/2, 0). Because this compound belongs to a body-centered tetragonal system, the calculation was performed on the primitive unit cell to minimize computational time. The Brillouin zone is shown in Figure S1. The energy scale is defined so that Fermi energy corresponds to zero energy. The fatband diagram[16] on the left-hand side shows the orbital contribution of Bi $6p_x$ and $6p_y$ orbitals. The partial density of states is shown on the right-hand side.

La_2O_2Bi. O 2p orbitals do not mix with either Bi 6s or 6p orbitals, because there are no Bi—O contacts in the structure, but they do mix to a small degree with neighboring La 5d orbitals. The La 5d/4f orbitals are located in the region of 1.9—5 eV, and these orbitals are mostly empty, again indicating that the La ion approximately adopts the trivalent state (La $5d^04f^0$) in La_2O_2Bi. Bi 6s and 6p levels do not mix with La 5d because of the longer La—Bi distance of 3.68 Å, compared with that in LaBi (3.28 Å),[15] even though these ions connect to each other directly. Bi 6p levels do not mix with Bi 6s because of the large difference of energy levels. These findings indicate that the Bi^{2-} layer governs the electronic structure near E_F and the 6p band is 83% (= 5/6) filled with electrons, because Bi^{2-} has an electronic configuration of $6s^26p^5$. The fatband description (vertical pink lines in Figure 3)[16] shows that the Bi $6p_x6p_y$ orbitals make a large contribution to the two widely spaced bands near E_F with a bandwidth of 3.5 eV. These two bands are highly dispersed along the symmetry lines ΓX and PN (which are along the *a*-direction) and are almost flat along the symmetry lines, ZΓ and XP (which are along the *c*-direction). The widths of these bands are sensitive to the *a*-value (that is, the Bi—Bi distance). Another band assigned to be Bi $6p_z$ exhibits almost no dispersion within the *ab* plane, resulting in a sharp DOS peak at −1.5 eV. This band is fully occupied in k-space, and does not contribute to the Fermi surface. Thus, the Fermi surface is 2D and composed of Bi $6p_x6p_y$. The orbital interactions associated with Bi are also shown in Figure 3, and these p—p σ interactions dominate the band dispersion near E_F and are often seen for square nets formed by s/p orbitals.[5,17]

The temperature dependence of the normalized electrical resistivity and Seebeck coefficient of the R_2O_2Bi compounds are shown in Figure 4. The resistivities are in the order of 10^{-3} ohm·cm. All of the samples show positive Seebeck coefficients,

dx.doi.org/10.1021/ja111015p | J. Am. Chem. Soc. 2011, 133, 2394–2397

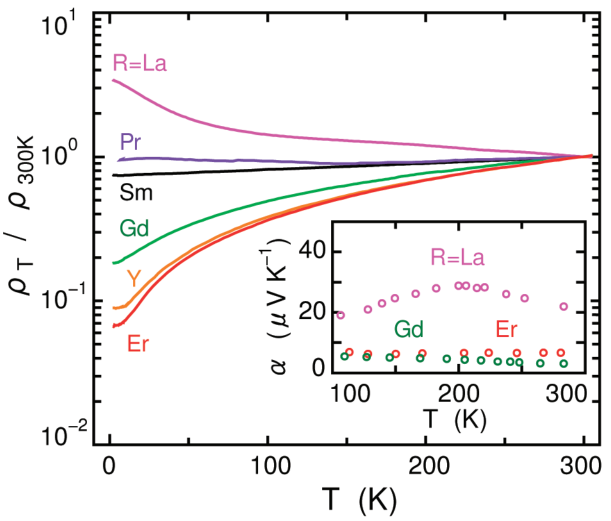

Figure 4. Temperature dependence of the normalized electrical resistivity (ρ) of R_2O_2Bi compounds. The inset shows the temperature dependence of the Seebeck coefficients (α).

indicating p-type conduction, which is consistent with the results of the band structure calculation (Figure 3). The resistivities of La_2O_2Bi show semiconducting behavior with a negative temperature coefficient, while those of Pr_2O_2Bi and Sm_2O_2Bi are almost independent of temperature. For small R ions, the resistivity of R_2O_2Bi shows metallic behavior, but no superconductive transition was observed down to 1.8 K. The observed MIT is caused by the size of the R ion decreasing. The contraction of the *a*-value from 4.08 Å (La_2O_2Bi) to 3.85 Å (Er_2O_2Bi) enhances the Bi 6p−Bi 6p σ bonding within the Bi^{2-} layer, which dominates the electronic structure near E_F. In other words, the width of the Bi 6p σ band crossing E_F can be controlled by chemical pressure using the size of the R ion. For La_2O_2Bi with a = 4.08 Å, the relatively narrow Bi 6p band is insufficient to maintain a good metallic state, although the band structure calculation of La_2O_2Bi suggests a metallic electronic structure. We think that the R_2O_2Bi system is a good platform from which to investigate the properties of the unusual Bi^{2-} ion. The temperature dependence of the magnetic susceptibility of R_2O_2Bi estimated using a vibrating sample magnetometer is shown in Figure S2. For Y_2O_2Bi and La_2O_2Bi, temperature-independent magnetic susceptibility, or Pauli paramagnetism, is observed over the whole temperature range. For Pr_2O_2Bi, Gd_2O_2Bi, or Er_2O_2Bi, the magnetic susceptibility increases with decreasing temperature (Curie−Weiss behavior), and it shows a cusp related to the antiferromagnetic transition because of the ordering of the R $4f^n$ spin under 15 K. The magnetic parameters obtained from the modified Curie−Weiss equation, $\chi = \chi_0 + C/(T - \theta)$ are summarized in Table S3. The effective Bohr magneton values, P_{eff}, for Pr_2O_2Bi, Gd_2O_2Bi, and Er_2O_2Bi were 3.70, 7.90, and 9.90 μ_B, respectively. These values agree well with the theoretical effective Bohr magneton values of 3.58, 7.94, and 9.59 for Pr^{3+}, Gd^{3+}, and Er^{3+}, respectively, indicating that the R ions are in a trivalent state. These results support the chemical formula of $R^{3+}{}_2O^{2-}{}_2Bi^{2-}$ in these compounds.

It was considered if R_2O_2Bi contains an effective Bi−Bi chemical bond. The Bi−Bi bond distance in elemental Bi (space group, R-3m) is 3.07 Å.[18] A bond length of ∼3.2 Å is found in Bi^- square nets such as those in $SrMnBi_2$, $BaZnBi_2$, and $LaLiBi_2$.[4−6] Thus, it is reasonable to consider that the observed Bi−Bi distance of 3.85−4.08 Å in R_2O_2Bi is too long for an effective chemical bond to form. The Bi array confined into the space between the two La_2O_2 layers is strongly constrained by the size of the La_2O_2 layer. Thus, an expanded square net of Bi is realized irrespective of no effective Bi−Bi bonding, and a relatively large bandwidth of Bi $6p_x6p_y$ of 3.5 eV is still realized for La_2O_2Bi, which has the largest *a*-value. The two-dimensional electronic structure formed by Bi $6p_x6p_y$ is clearly shown in the band calculation depicted in Figure 3.

It is unusual that the MIT occurs in a square net of main group (p-block) elements. Because of this, the origin of the MIT was considered. A square net of 5p elements such as Sb or Te is often distorted to form a zigzag chain within the layer to reduce the DOS at E_F.[5,19] The driving force for this is the Jahn−Teller effect. On the other hand, this kind of distortion does not usually occur in Bi compounds.[5] The stabilization energy caused by the delocalization of the hole may be larger than that caused by the Jahn−Teller effect. For La_2O_2Bi, the increase of the *a*-value without the reduction of crystal symmetry makes the bandwidth of Bi $6p_x6p_y$ narrow, and as a result, the mobility of the positive hole decreases. This effect may be categorized as a Mott transition that is induced by the chemical pressure exerted by changing the size of the R ion.

■ ASSOCIATED CONTENT

Ⓢ Supporting Information. Crystal structure parameters, magnetic susceptibilities. This material is available free of charge via the Internet at http://pubs.acs.org.

■ AUTHOR INFORMATION

Corresponding Author
hosono@lucid.msl.titech.ac.jp

■ ACKNOWLEDGMENT

This work was supported by the Funding Program for World-Leading Innovative R&D on Science and Technology (FIRST), Japan. We thank Prof. O. K. Andersen and Dr. O. Jepsen (Max Plank Institute, Stuttgart, Germany) for providing us with the LMTO code. We are also grateful to Prof. Masahiro Hirano (Tokyo Inst. Tech.) for helpful discussions.

■ REFERENCES

(1) (a) Bednorz, J. G.; Muller, K. A. *Z. Phys. B* **1986**, *64*, 189. (b) Kamihara, Y.; Watanabe, T.; Hirano, M.; Hosono, H. *J. Am. Chem. Soc.* **2008**, *130*, 3296.

(2) (a) Sleight, A. W.; Gillson, J. L.; Bierstedt, P. E. *Solid State Commun.* **1975**, *17*, 27. (b) Mattheiss, L. F.; Gyorgy, E. M.; Johnson, D. W. *Phys. Rev. B* **1988**, *37*, 3745.

(3) Hasegawa, A. *J. Phys. Soc. Jpn.* **1985**, *54*, 677.

(4) (a) Cordier, G.; Schafer, H. *Z. Naturforsch, B: Chem. Sci.* **1977**, *32*, 383. (b) Brechtel, E.; Cordier, G.; Schafer, H. *Z. Naturforsch, B: Chem. Sci.* **1980**, *35*, 1. (c) Brechtel, E.; Cordier, G.; Schafer, H. *J. Less-Common Metals* **1981**, *79*, 131. (d) Zelinska, O. Y.; Ma, A. *J. Alloys Cmpd.* **2008**, *451*, 606.

(5) Tromel, W.; Hoffmann, R. *J. Am. Chem, Soc* **1987**, *109*, 124.

(6) Pan, D.; Sun, Z.; Mao, J. *J. Solid State Chem.* **2006**, *179*, 1016.

(7) Papoian, G. A.; Hoffmann, R. *Angew. Chem., Int. Ed.* **2000**, *39*, 2408.

(8) Mizoguchi, H.; Matsuishi, S.; Hirano, M.; Tachibana, M.; Takayama-Muromachi, E.; Kawaji, H.; Hosono, H. *Phys. Rev. Lett.* **2011**, *106*, 057002.

(9) Benz, R. *Acta Crystallogr., Sect. B* **1971**, *27*, 853.

(10) Nuss, J.; Jansen, M. *J. Alloys Cmpd.* **2009**, *480*, 57.

(11) The Cu rotation anode in our diffraction system is slightly contaminated by W-filament, and the radiation includes a very small amount of W Lα. The intensity ratio, Cu Kα/W Lα is refined in the fitting process.

(12) *TOPAS*, version 3; Bruker AXS: Karlsruhe, Germany, 2005.

(13) Shannon, R. D. *Acta Crystallogr., Sect. A* **1976**, *32*, 751.

(14) Andersen, O. K.; Jepsen, O. *Phys. Rev. Lett.* **1984**, *53*, 2571.

(15) Nomura, K.; Hayakawa, H.; Ono, S. *J. Less-Common Metals* **1977**, *52*, 259.

(16) "Fatband" are used to highlight the individual orbital contributions to each band. The width of the hatching corresponds to the amount of contribution of a particular atomic orbital to the band in question. Fatbands are a useful tool to quantify the change in orbital contribution from band to band, and within a given band, as one moves through reciprocal space.

(17) Hoffmann, R. *Solids and Surfaces: A Chemist's View of Bonding in Extended Structures*; VCH: New York, 1988; Chapter 8.

(18) Cucka, P.; Barrett, C. S. *Acta Crystallogr.* **1962**, *15*, 865.

(19) Wang, Y. C.; Poduska, K. M.; Hoffmann, R.; DiSalvo, F. J. *J. Alloys Cmpd.* **2001**, *314*, 132.